PHYS 3081 Lab Report: Gamma-Ray Crystal Spectrometer Experiment*

Vytis Krupovnickas† and Ari Moscona‡
Columbia University
538 W 120th St, New York, NY 10027

Vytis Krupovnickas§
Columbia University

Ari Moscona
Columbia University

(Dated: September 15, 2023)

In this experiment, we used a gamma-ray crystal spectrometer to investigate gamma ray interactions with a Sodium Iodide (NaI) scintillation crystal. We employed a photomultiplier tube (PMT) to convert emitted light into electrical pulses. Our methodology consisted of observing output pulses from various gamma-ray sources; using a pulse height analyzer to measure gamma-ray energy peaks; determining the energy resolution of the photocathode; and detecting fluorescent x-rays from known substances. Identifying an 'unknown' target by measuring its fluorescent x-rays.

We calibrated and analyzed the spectrometer data, establishing a linear energy relation for gamma-rays. We verified the Compton edge and backscattering peak energies using Compton scattering kinematics. We created nuclear energy level diagrams for observed gamma-ray transitions. Our analyses yielded two detector constants (A and C), the number of photoelectrons per MeV (NPE), and the photocathode quantum efficiency. We compared Kα x-ray energies against Moseley's Law $(Z-1)^2$. This experiment enhanced our understanding of gamma-ray interactions, photomultiplier tube operations, and NaI detector spectroscopic properties.

I. INTRODUCTION

This experiment represents a significant milestone in the pursuit of understanding the behavior of gamma rays, scintillation crystals, and the photoelectric effect. This laboratory report outlines the principles, procedures, and analyses undertaken during the Gamma-Ray Crystal Spectrometer Experiment.

The Gamma-Ray Crystal Spectrometer experiment explores the interactions between gamma rays and NaI (sodium iodide) crystals, investigating the properties of gamma radiation, energy resolution, and the quantum efficiencies of critical detector components. The knowledge gained from this experiment not only enriches our comprehension of nuclear physics but also has practical applications in fields such as radiation detection and nuclear particle physics. The Gamma-Ray Crystal Spectrometer experiment provides an opportunity to study the interactions of high-energy gamma rays with matter, shedding light on the fundamental behavior of subatomic particles. Understanding how gamma rays are absorbed, scattered, and detected within NaI crystals contributes to our comprehension of the atomic and nuclear structure, as well as the forces that govern these interactions.

The core principle of the Gamma-Ray Crystal Spectrometer experiment centers around the interaction of energetic gamma rays with NaI crystals. When a gamma ray is completely absorbed within the crystal, it imparts its energy to electrons through Compton scattering and the photoelectric effect. These electrons subsequently undergo ionizing collisions within the crystal, losing energy until they reach their ground state. A fraction of the energy lost in this process is emitted as visible light, a phenomenon known as scintillation. Approximately 8700 visible photons are emitted for every MeV of energy loss, making NaI crystals efficient detectors.

The transparent NaI crystal is optically coupled to a photomultiplier tube in order to analyze the light emitted during scintillation. The photocathode within the photomultiplier emits electrons in response to incident photons, initiating a cascade of electron multiplication through a series of dynodes. This process culminates in a pulse of current at the anode, providing a measurable signal that corresponds to the energy of the incident gamma ray.

One crucial aspect of the Gamma-Ray Crystal Spectrometer experiment is the determination of energy resolution, or the quantum efficiency of the cathode, denoted as ΔE/E, which quantifies the variation in output current pulses for gamma rays of energy E. This resolution is influenced by statistical fluctuations in the number

---

* Performed in Pupin Laboratories under supervision of Morgan May
† Also at Physics Department, Columbia University.
‡ adm2192@columbia.edu
§ vtk2105@columbia.edu

of photoelectrons emitted by the photocathode (NPE). The energy resolution, expressed as the full width at half maximum (FWHM), is integral to understanding the accuracy and precision of gamma-ray measurements, as it determines the rate at which incident gamma photons are converted to electrons through scintillation.

In the following sections, we will detail the theory, equipment, experimental procedure, data analysis, and conclusions drawn from the Gamma-Ray Crystal Spectrometer Experiment. We aim to expand our understanding of gamma-ray interactions, nuclear physics, and radiation detection technologies.

II. THEORY

Cesium-137 is an isotope of Cesium which is produced from the decay of Uranium-235. Approximately 94.6% of Cesium-137 decays (Equation 1) into Barium-137 through beta-emission, producing a distinct low-energy peak in the energy spectrum. The decay produces a meta-stable Barium-137 nuclear isomer, which recombines into a stable state which in turn produces an x-ray fluorescence peak on the graph at lower energy bins. Barium-137 produces gamma-ray emissions, which are detected adjacent to the Cesium-137 beta decay peak.

$$^{137}_{55}\mathrm{Cs} \rightarrow ^{137}_{56}\mathrm{Ba} + e^- + \overline{\nu}_e \tag{1}$$

Sodium-22 is an isotope of Sodium which decays (Equation 2) through beta decay to Neon-22. This excited state of neon passes into the ground state by emitting a highly energetic gamma ray. The positrons (beta decay) emitted from Sodium-22 decay also interact with electrons in surrounding matter. The positron-electron annihilation produced from this interaction creates two gamma quanta also seen in the spectrum.

$$^{22}_{11}\mathrm{Na} \rightarrow ^{22}_{10}\mathrm{Ne} + e^+ + \nu_e \tag{2}$$

Thallium-204 is a synthetic isotope of Thallium, usually manufactured in a cyclotron - a circular particle accelerator which accelerates particles through an electromagnetic field, allowing for probes to be placed inside to produce radionuclides - which decays (Equation 3) through beta decay directly into Lead-204 or beta decay and electron capture into Mercury-204.

$$^{204}_{81}\mathrm{Tl} \rightarrow ^{204}_{82}\mathrm{Pb} + e^- + \overline{\nu}_e \tag{3}$$

Strontium-90 is an isotope of Strontium which decays (Equation 4)through beta decay into Yttrium-90, an electron, and an antineutrino. The Yttrium isotope then further decays by beta emission into an electron, antineutrino, and Zirconium-90, which is stable.

$$^{90}_{38}\mathrm{Sr} \rightarrow ^{90}_{39}\mathrm{Y} + e^- + \overline{\nu}_e \rightarrow ^{90}_{40}\mathrm{Zr} + e^- + \overline{\nu}_e \tag{4}$$

Cobalt-60 is a synthetic isotope of cobalt which decays (Equation 5) via beta decay into Nickel-60. The activated nickel isotope then emits two gamma rays (Equation 6) of differing energies in order to reach a stable form.

$$^{60}_{27}\mathrm{Co} \rightarrow ^{60}_{28}\mathrm{Ni} + e^- + \bar{\nu}_e \tag{5}$$

$$^{60}_{28}\mathrm{Ni} \rightarrow ^{60}_{28}\mathrm{Ni} + \gamma + \gamma \tag{6}$$

Compton scattering is the process by which electromagnetic waves are scattered when they have been scattered by electrons. The photons have energy and momentum as particles do; when collisions occur with electrons, they can be described by equation 7, which describes the final-state energy ($E_{\gamma'}$) of the photon as a function of its incident energy (E_γ) and scattering angle. When individual photons collide with electrons, they transfer some of their energy and momentum to the electron, causing some recoil. During the collision, other photons are produced with less energy and momentum than the colliding photon, which are scattered at angles dependent on the amount of energy lost by the recoiling electron.

$$E_{\gamma'} = \frac{E_\gamma}{1 + \frac{E_\gamma}{mc^2}(1 - cos(\theta))} \tag{7}$$

The resolution of the detector is calibrated according to Poisson statistics, as the detector measures low counts. The Poisson distribution assumes that events occur independent of each other over a certain time interval, and that these time intervals can be described discretely in whole integer values. Additionally, it is assumed these events do not occur at the same instant, instead occurring (or not occurring) at small sub-intervals. This makes the Poisson distribution ideal for describing the number of decay events from radioactive sources, which follow this rule over the time periods they are observed.

III. METHODOLOGY AND DESCRIPTION

A. Equipment

The oscilloscope (Figure 1) is a device which is used for visualizing and analyzing electrical signals over time. The screen (usually a CRT screen) is divided by horizontal and vertical lines called the graticule, against which a waveform is measured. The vertical selection controls for the amplitude of the display signal, while the horizontal selection controls for the time over which the signal is observed. The oscilloscope is used to get a general overview of the energy emission spectrum of the observed radioactive source.

The photocathode tube sodium iodide scintillation detector (Figure 2) is designed to detect and measure ionizing radiation, such as gamma and x-rays, by converting the energy of incoming radiation into visible light,

FIG. 1. LeCroy WAVEACE 101 40 MHz, 2 Channel Digital Oscilloscope, from tequipment.net

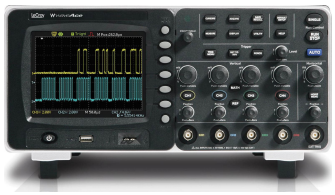

which can then be detected and analyzed. When ionizing radiation hits the crystal, its energy is transferred to it, causing the atoms in the crystal to become temporarily excited before emitting photons as they return to the ground state. The photons are then emitted into a photocathode (a material sensitive to visible light) which causes an emission of electrons via the photoelectric effect. The number of emitted electrons is proportional to the number of photons hitting the photocathode, which is proportional to the energy of the incident radiation. This information is translated to and by the multi channel analyzer to the CAEN software on the computer.

FIG. 2. Scionix 38B57 1.5"x2.25" NAI(Tl) Gamma Scintillation Detector Probe, from scionix.nl

The dual digital multi channel analyzer (figure 3) serves multiple functions within the setup. The multichannel analyzer portion of the device digitizes and analyzes signals from the photocathode tube. It processes the incoming analog signals, converting them into digital data that can be used for spectral analysis. It accumulates data on the energies of detected radiation events, creating an energy spectrum. The device provides a stable high voltage supply to power the radiation detectors and preamplifiers, a device which amplifies the early signal, reducing background noise. This ensures that the detectors operate at their optimal sensitivity and performance levels.

FIG. 3. Dual Digital Multi Channel Analyzer (Preamplifier PS) - Desktop, from caen.it

B. Method

First, the power supply is turned on and connected to the photomultiplier tube. One of the radiation sources is placed at the end of the photomultiplier tube, then covered by a dense material behind to "muffle" background radiation. The radiation source is analyzed qualitatively by observing the energy spectra and their peaks through an oscilloscope (Figure 1). Then, spectral features, pulse heights of full-energy peaks, and upper Compton edges are observed and recorded (Figures 5-8).

IV. DATA

A. Data Analysis

The channel number and counts are calibrated to absolute energy values according to equation 8, using the highly energetic gamma ray peaks of Sodium-22 and the low-energy x-ray fluorescence peaks of the Cesium-137 energy spectrum. In Equation 8, E_γ is the energy of the gamma ray (in eV), g is the gain, which refers to the linear increase in energy per channel, C is the channel number, and o is the offset of the energy per channel. The slope and offset is calculated through using the experimentally accepted energies of the x-rays emitted from the Cesium-137 source and Sodium-22 gamma ray emission during its decay, and using the centroid of those gamma emission peaks we obtained during our experiment. The resulting calibration is graphed in Figure 4.

$$\{E_\gamma = gC + o\} \tag{8}$$

The gamma ray peaks are obtained from the peak height analyzer included in the CAEN software. This allows to easily find the centroid as well as the full-width half maximum of the peak and resolution for each observed emission. The CAEN software graphs are shown in Figures 5-8. The graphs display channel number versus counts.

FIG. 4. Energy Calibration Graph. Note the gain of 2.899 and offset is -36.16. The centroid for each peak is graphed against the gamma energy.

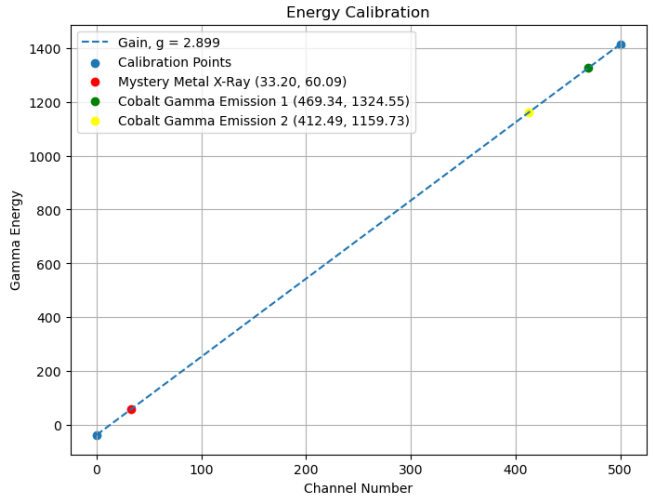

FIG. 5. Sodium-22 Energy Spectrum. Note the furthest right peak shows the gamma ray emission with a photon valley adjacent to it, and a large peak showing the beta emission from initial sodium-22 decay.

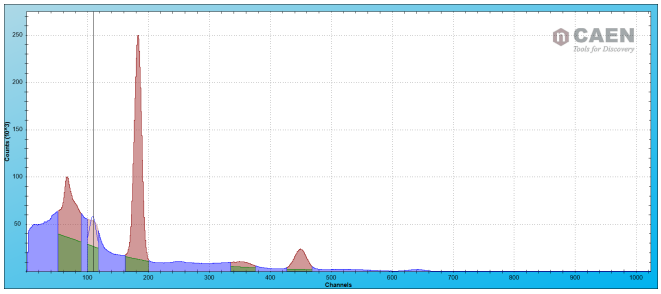

FIG. 6. Cobalt-60 Energy Spectrum. The furthest right peaks are the two gamma ray emissions from cobalt-60 decay, with two overlapping compton backscattering peaks adjacent to it. A beta decay peak can be seen at the far left.

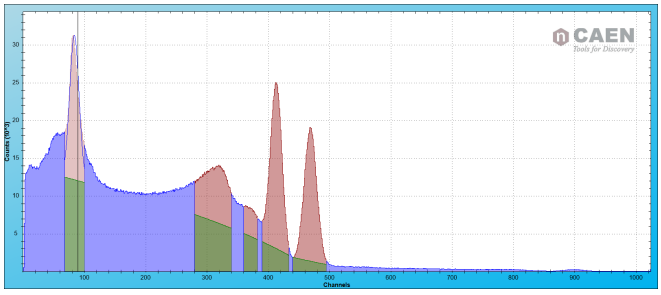

The energy level diagrams for the Sodium-22, Cobalt-60, and Cesium-137 are shown in Figures 9-11. We used the energy values for Sodium-22 gamma ray emission and Cesium-137 x-ray emission as our accepted values for the energy calibration. Furthermore, the energy spectra for Thallium-204 and Strontium-90 are shown in the Appendix (Figures 13 and 14), although they were not analyzed as they only exhibit beta decay.

FIG. 7. Cesium-137 Energy Spectrum. The rightmost peak shows the gamma ray emission from Cesium-137 decay, with a compton backscattering peak to its left. The furthest left peak shows the x-ray flourescence emission from Barium-137 recombination to a stable energy state.

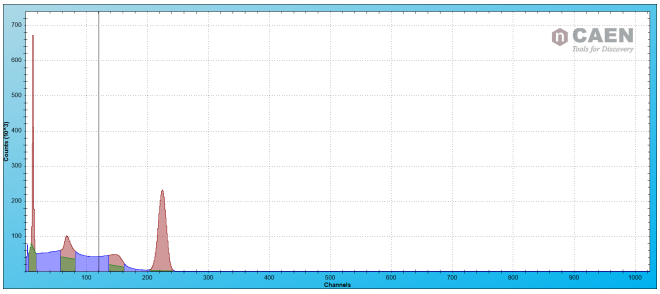

FIG. 8. Mystery Metal Energy Spectrum. The major wave forms are products of the background emissions and nearby Cobalt-57 source used to excite x-rays from the mystery metal. The large peak second from the left is the emitted x-rays from the mystery metal.

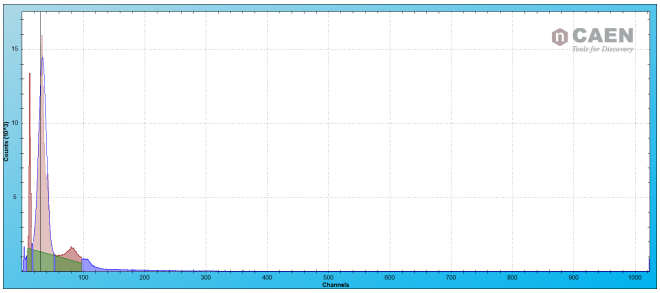

FIG. 9. Sodium-22 Energy Level Diagram, from physicsopenlab.org

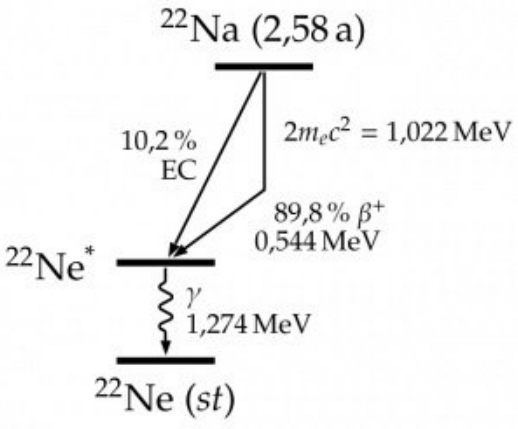

FIG. 10. Cobalt-60 Energy Level Diagram, from wikipedia.org

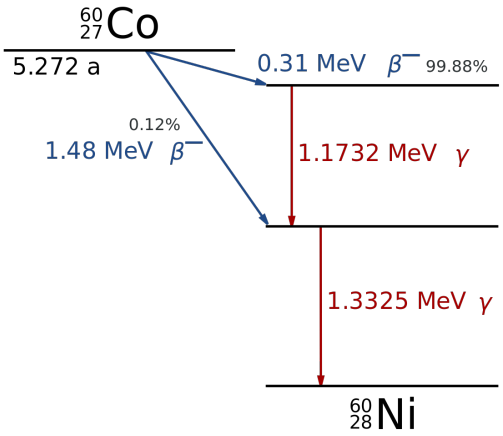

FIG. 11. Cesium-137 Energy Level Diagram, from maximus.energy

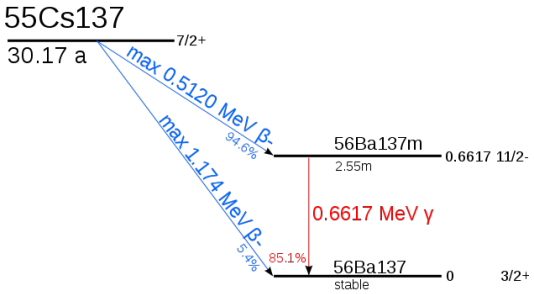

B. Quantum Efficiency of Cathode

The energy resolution (ΔE) of a scintillation crystal is a parameter which quantifies the efficiency at which an incident photon from a gamma ray source is converted to an electron in the photomultiplier. This is important for getting a higher energy resolution - as we receive more electrons per gamma ray collision - which gives more accurate energy readings for our calibrations. The energy resolution is determined by the statistical fluctuation in the number of photoelectrons emitted by the photocathode, or the N_{PE}. The standard deviation of N_{PE} is expressed as $\sigma(N_{\mathrm{PE}}) = \sqrt{A * E * N_{\mathrm{PE}}}$, where A is a constant of the detector. The relationship between the statistical uncertainty, number of incident particles, gamma energy E, and A is shown in equation 9.

Other factors contribute a constant term C to the energy resolution (ΔE/E) that does not depend on the gamma ray's energy E. The constants A and C combine to determine the total energy resolution (Equation 10). The energy resolution is defined by the full width half-maximum (FWHM), which is defined by the equation $\Delta E/E = \frac{FWHM}{2.4}$.

$$\frac{\Delta E}{E} = \frac{\sigma(N_{\mathrm{PE}})}{N_{\mathrm{PE}}} = \frac{\sqrt{N_{\mathrm{PE}}}}{N_{\mathrm{PE}}} = \frac{A}{\sqrt{E}} \tag{9}$$

We can use equation 10 to get the quantum efficiency ($(\frac{\Delta E}{E})^2$) of the cathode. We solve for the constants A and C in Equation 10 using the FWHM of the low energy x-ray of Cesium-137 and high energy gamma ray of Sodium-22, the values of which are plotted as $(\frac{\Delta E}{E})^2$ versus $\frac{1}{E}$ in figure 12. Given the values described in Table 1, we determined A = 0.14 and C = 0.41.

$$(\frac{\Delta E}{E})^2 = (\frac{A}{\sqrt{E}})^2 + C^2 \tag{10}$$

FIG. 12. Quantum Efficiency of Cathode Graph

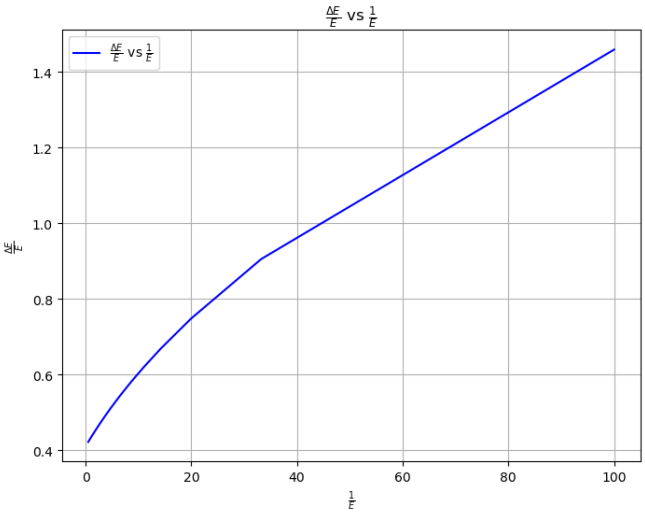

C. Compton Scattering

When energetic x- and gamma rays are emitted from a radioactive source, they will be emitted 360 degrees around the source. When these rays collide with the crystal, they will collide with relativistic momentum and scatter, similar to billiard balls. This scattering can be seen on the energy spectra graphs in Figures 5-7 as peaks to the left of gamma ray emissions separated by a valley. This valley represents all of the photons which completely reflect away at 180 degrees during the collision, which the Compton scattering are those which collide at differing angles and are absorbed by the crystal.

We look at the Compton edge - the point of maximum energy transfer, where the particle is completely deflected 180 degrees after collision with an electron at rest mass in the crystal - for the energetic gamma rays emitted by sodium-22, cesium-137, and cobalt-60. The centroids of the Compton edge are provided in table 3. The Compton

edge is the maximum amount of energy transferred to an electron of rest mass 511 keV. in the NaI scintillation crystal. Using equation 7, we can calculate the energy and thus the channel we predict the Compton edge will be, which is the point at which incoming gamma rays are deflected 180 degrees. The values of the Compton edge energy are included in Table 3. We find that the calculated Compton edges closely match the identified peaks.

D. Data

TABLE I. The centroids, FWHM, and resolutions of the four measured sources are listed in the table.

Source	Centroid	FWHM	Resolution
Na-22	449.52	14.32	6.38%
Co-60 γ-ray 1	469.34	22.25	4.75%
Co-60 γ-ray 2	412.49	21.01	5.09%
Cs-137 γ-ray	224.38	14.32	6.38%
Cs-137 x-ray	12.7	2.44	19.21%
Myst. Metal	33.20	14.51	60.09%

TABLE II. The centroids and gamma rays from each source are listed in the table below.

Source	Centroid	Energy (keV)
Na-22	449.52	1275
Co-60 γ-ray 1	469.34	1324.55
Co-60 γ-ray 2	412.49	1159.73
Cs-137 γ-ray	224.38	614.36
Cs-137 X-ray	12.7	0.66
Myst. Metal	33.20	47.62

TABLE III. The centroids and energy of the associated centroid for the compton edge from each source are listed in the table below.

Source	Centroid	Act. Energy (keV)	Exp. Energy (keV)
Na-22	279.13	773.1	1062.15
Co-60 γ-ray 1	371.17	1039.93	1110.37
Co-60 γ-ray 2	311.41	866.68	950.36
Cs-137 γ-ray	148.59	394.63	433.91

V. DISCUSSION

The values we obtained during on experiment are listed in Table 1 and Table 2. We used the theoretical gamma ray emission energy for sodium-22 and cesium-137 in order to perform our energy calibrations, and, using these values, calculated the values for cobalt-60's two gamma ray emissions as well as the x-ray fluorescence obtained for the mystery metal. The theoretical value for the emission energy of cobalt-60's gamma rays are 1.17 MeV and 1.33 MeV, our obtained values were 1.16 MeV and 1.32 MeV. These values very closely match the theoretical value, and thus we can be confident with our calibration, especially when accounting for the reduced quantum efficiency of the photocathode at more energetic emissions.

The mystery metal's x-ray emission energy was 60.09 keV. Using this information, we can determine that the mystery metal is likely lanthanum. Lanthanum emits x-rays of energy 33.44 keV. Our result is significantly different from this, but this is due to our calibration being performed using very high energy gamma rays, giving us an upward skew for our calibration. For higher energies our results are more accurate; for lower energies, our results will be linearly off from the actual energy of observed rays. Thus, lanthanum most closely matches the energy measured from the mystery metal.

A. Errors

Due to the age of the samples, a larger portion of the radiation source has already decayed into more stable isotopes, thus reducing observed emissions. Additionally, based on the calculations for the quantum efficiency of the cathode, we understand that the efficiency declines for smaller energies. Thus, for low energy gamma rays, the data will not as closely match the accepted energies of gamma rays emitted during decays.

VI. CONCLUSION

We learned from this experiment how to analyze the energy spectra of various radioactive metals, recognizing the different types of observed emissions. We analyzed not only the decay of atoms within the samples, but their energies and how the energetic rays emitted interact physically with the set up. We additionally learned the theory behind the photocathode ray tube, how quantum efficiency is calculated, its importance in obtaining accurate measuremnts, the visual representation of Compton scattering in the energy spectrum, and the methods by which substances may be identified as well as counting statistics necessary for understanding and interpreting the obtained data.

The lab could be expanded upon by using different radioactive substances emitting gamma and x-rays at many different energies in order to create a stronger energy calibration. More unknown materials could be analyzed in order to expand students' knowledge of characteristic energy spectra, allowing them to work with elements more effectively. I would recommend this lab as it was useful for gaining insight into how photomultipliers work and the energy spectra of easily recognizable radioactive materials.

VII. REFERENCES

Fermi. E., Nuclear Physics; reprint- Compton scattering, photoelectric effect, Moseley's Law.

W.R. Leo, Techniques for Nuclear and Particle Physics Experiments, Springer-Verlag 1994. Chapter 1 for a discussion of β decay, gamma emission, annihilation radiation, internal conversion, etc.

Knoll, G. F., Radiation Detection and Measurement (1989) Chapter 8 II; Chapter 9 I,II Photomultipliers; Chapter 10 I-IV - Detector properties. Chapter 18 first few pages- Multichannel analyzer.

Handbook of Chemistry and Physics. Lederer C. and Shirley V., Table of Isotopes.

Appendix A: Graphs

FIG. 13. Thallium-204 Energy Spectrum

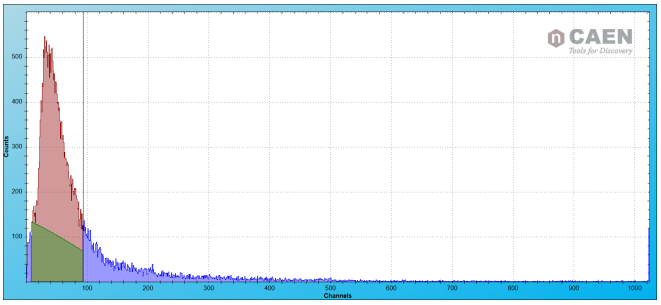

FIG. 14. Strontium-90 Energy Spectrum